Journal of Thermal Analysis and Calorimetry, Vol. 94 (2008) 1, 219–226

XRD, TEM AND THERMAL ANALYSIS OF YTTRIUM DOPED BOEHMITE NANOFIBRES AND NANOSHEETS

Y. Zhao[1], *R. L. Frost*[1*], *Veronika Vágvölgyi*[2], *E. R. Waclawik*[1], *J. Kristóf*[2] *and Erzsébet Horváth*[3]

[1]Inorganic Materials Research Program, School of Physical and Chemical Sciences, Queensland University of Technology 2 George Street, GPO Box 2434, Brisbane, Queensland 4001, Australia
[2]Department of Analytical Chemistry, University of Pannonia, 8201 Veszprém, PO Box 158, Hungary
[3]Department of Environmental Engineering and Chemical Technology, University of Pannonia, 8201 Veszprém PO Box 158, Hungary

Yttrium doped boehmite nanofibres with varying yttrium content have been prepared at low temperatures using a hydrothermal treatment in the presence of poly(ethylene oxide) surfactant (PEO). The resultant nanofibres were characterized by X-ray diffraction (XRD) and transmission electron microscopy (TEM). TEM images showed the resulting nanostructures are predominantly nanofibres when Y-doping is less than 5%; in contrast Y-rich phases were formed when doping was around 10%.

The doped boehmite and the subsequent nanofibres/nanotubes were analyzed by thermogravimetric and controlled rate thermal analysis methods. The boehmite nanofibres produced in this research thermally transform at higher temperatures than boehmite crystals and boehmite platelets. Boehmite nanofibres decompose at higher temperatures than non-hydrothermally treated boehmite.

Keywords: *acicular, boehmite, nanofibre, nanomaterial, nanosheets, nanotube*

Introduction

Recently, the synthesis of inorganic nanoscale materials with special properties has been of great interest in material science [1, 2], because their intrinsic properties at the nanoscale level. Material properties are mainly determined by their composition, structure, crystallinity, size and morphology [3]. In particular, one dimensional (1D) nanoscale inorganic materials including nanofibers, nanowires and nanotubes have attracted extensive interest due to their distinctive geometries, novel physical and chemical properties and potential applications in numerous areas [4].

Boehmite (AlOOH), a principal oxo-hydroxide of aluminium, is a crucial precursor in sol–gel technique for preparing high-purity and high-strength monolithic α-alumina ceramics for use as substrates for electronic circuits, abrasive grains, high-temperature refractory materials, fibres and thin films [5]. Alumina (Al_2O_3) can be obtained from AlOOH by a simple dehydration process from a certain temperature. It has been demonstrated that AlOOH nanostructures undergo an isomorphous transformation to nanocrystalline alumina during heating [6–8]. Therefore, the morphology and size of the resultant alumina can be manipulated by controlling the growth of boehmite. Alumina has been employed as catalyst [9], adsorbent [10, 11], composite materials [12, 13] and ceramics [14–16]. Due to the high surface area of alumina phases, its chemical and thermally stable properties and mesoporous properties, alumina has been extensively used as carrier and support for a variety of industrial catalysts at high temperature as well as low temperature. It is believed that the high temperature creep deformation of alumina is related to the grain boundary diffusion process in polycrystalline alumina [17]. It has been noticed that high-temperature creep in fine-grained alumina can be controlled by doping with small amounts of rare-earth elements, such as yttrium [18]. Besides, doped with yttrium, the resulting boehmite/alumina nanostructure may have special optical properties which will enable it to further industrial applications.

Thermal analysis has proved most useful for the analysis of minerals and related materials [19–28]. In this work, a series of yttrium doped boehmite nanofibres with varying yttrium content have been synthesised by introducing yttrium as dopant and the properties of the resultant yttrium doped boehmite nanofibres were systematically studied using X-ray diffraction, transmission electron microscopy and both dynamic and controlled rate thermogravimetric techniques.

Experimental

Synthesis of Y-doped boehmite nanofibres

The detailed experimental procedure is as follows. A total amount of 0.2 mol aluminium nitrate and

* Author for correspondence: r.frost@qut.edu.au

1388–6150/$20.00

Akadémiai Kiadó, Budapest, Hungary
Springer, Dordrecht, The Netherlands

yttrium nitrate were mixed before dissolved in ultra-pure water. Mixtures with yttrium molar percentage of 1, 2, 3, 4.5 and 10% were prepared separately and then dissolved in ultra-pure water to form a solution (A) with a metal ion to H_2O molar ratio of 1:100 and heated to 80°C. With stirring in solution A, 5 mol L^{-1} NaOH solution was then added dropwise at a constant rate of 5 mL min^{-1} to form precipitate. After that it was aged for two hours with constant stirring at 80°C, the resulting precipitate was recovered by centrifugation, washed with pure water several times to remove sodium nitrate. The washed precipitate was then mixed with water and nonionic PEO surfactant Tergitol 15-S-7 ($C_{12-14}H_{25-29}O(CH_2CH_2O)_7H$, Aldrich) with average molecular mass of ~508 at a metal:H_2O:PEO molar ratio of 0.2:3.2:0.04. The viscous mixture is stirred for 1 h at room temperature and then transferred into an autoclave and kept in oven an at 100°C for 6-day hydrothermal treatment. The final product was washed by water and dried in air at 80°C.

X-ray diffraction

XRD analyses were performed on a PANalytical X'Pert PRO X-ray diffractometer (radius: 240.0 mm). Incident X-ray radiation was produced from a line focused PW3373/10 Cu X-ray tube, operating at 45 kV and 35 mA, providing $K_{\alpha 1}$ wavelength of 1.540596 Å. The incident beam passed through a 0.04 rad, Soller slit, a 1/2° divergence slit, a 15 mm fixed mask and a 1° fixed anti-scatter slit. After interaction with the sample, the diffracted beam was detected by an X'Celerator RTMS detector. The detector was set in scanning mode, with an active length of 2.022 mm. Samples were analysed utilising Bragg–Brentano geometry over a range of 3–75° 2θ with a step size of 0.02° 2θ, with each step measured for 200 s.

TEM analysis

A Philips CM 200 transmission electron microscopy (TEM) at 200 kV was used to investigate the morphology of the boehmite nanofibres. All samples were dispersed in absolute ethanol solution and then dropped on copper grids coated with carbon film, dried in an oven at 60°C for 10 min for TEM studies.

Thermal analysis

Dynamic experiment

Thermal decomposition of the yttrium doped boehmite samples was carried out in a Derivatograph PC-type thermoanalytical instrument (Hungarian Optical Works, Hungary) capable of recording the thermogravimetric (TG), derivative thermogravimetric (DTG) and differential thermal analysis (DTA) curves simultaneously. The sample was heated in a ceramic crucible in static air atmosphere at a rate of 5°C min^{-1}.

Controlled rate thermal analysis experiment

Thermal decomposition of the yttrium doped boehmite was carried out in a derivatograph in static air atmosphere (250 cm^3 min^{-1}) at a pre-set, constant decomposition rate of 0.15 mg min^{-1}. (Below this threshold value the samples were heated under dynamic conditions at a uniform rate of 1.0°C min^{-1}). The samples were heated in an open ceramic crucible at a rate of 1.0°C min^{-1}. With the quasi-isothermal, quasi-isobaric heating program of the instrument the furnace temperature was regulated precisely to provide a uniform rate of decomposition in the main decomposition stage.

Results and discussion

X-ray diffraction

Figure 1 shows the XRD patterns of doped samples after 6 days hydrothermal treatment at 100°C. All the diffraction peaks of the resultant samples with yttrium doping of 1, 2, 3, 4 and 5% can be assigned to orthorhombic boehmite (AlOOH, JCPDS 00-005-0190). The characteristic diffraction peaks for boehmite at around 14, 28, 38 and 48° 2θ degree indicate an excellent crystallinity of these samples. As for 10% doped sample, yttrium peaks as well as boehmite peaks were presented in the XRD pattern. Peak position, FWHM, lattice parameters and crystal sizes of samples with varying Y-content after 6 days hydrothermal treatment at 100°C are shown in Table 1. Peak position at both 020 and 002 varied with the increase in doped Y%. Variation in lattice parameter *b* was observed whereas lattice parameter *c* remains constant with the increase in Y-content when taking account of calculation errors. Crystallite size along *c* and *b* crystallographic directions varies with the increase in doped Y.

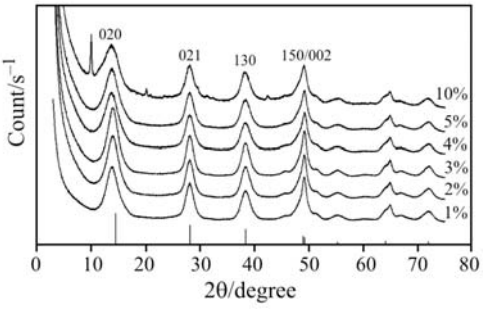

Fig. 1 Powder X-ray diffraction patterns of Y doped boehmite samples with varying Y%

Table 1 Peak position, FWHM, lattice parameters and crystal sizes of samples with varying Y-content after 6 days hydrothermal treatment at 100°C

Added/%	*h k l*	Peak position	FWHM	Lattice parameter/Å	Crystal size/nm
		2θ/degree			
1	0 2 0	13.820	2.222	12.81	3.6
	0 0 2	49.120	0.672	3.71	13.0
2	0 2 0	13.970	2.180	12.67	3.7
	0 0 2	49.178	0.894	3.70	9.8
3	0 2 0	13.990	1.998	12.65	4.0
	0 0 2	49.157	0.624	3.70	14.0
4	0 2 0	13.754	2.400	12.87	3.3
	0 0 2	49.192	0.726	3.70	12.0
5	0 2 0	13.795	2.386	12.83	3.4
	0 0 2	49.160	0.658	3.70	13.3
10	0 2 0	13.816	2.551	12.81	3.1
	0 0 2	49.115	0.883	3.71	9.9

Transmission electron microscopy

Figure 2 shows the morphology of Y-doped samples after 6 days hydrothermal treatment with Y% of 1, 3 and 5. It was noted that nanofibres, nanotubes with small amount of nanosheets were formed in all these three samples. The overall morphology and size of 1 and 3% doped boehmite are similar. The average length and width of these two samples are approximately 90 and 2.5 nm, respectively. It was noted that the size of 5% Y-doped boehmite was remarkable bigger than the other two doped samples with an average length and width of about 100 and 3.5 nm which is close to the size of pure boehmite synthesized under the same procedure and conditions our early study [29]. As for 10% sample, except for nanofibres with similar size as that formed in 5% sample, large nanorods and square-shaped yttrium rich crystals were observed.

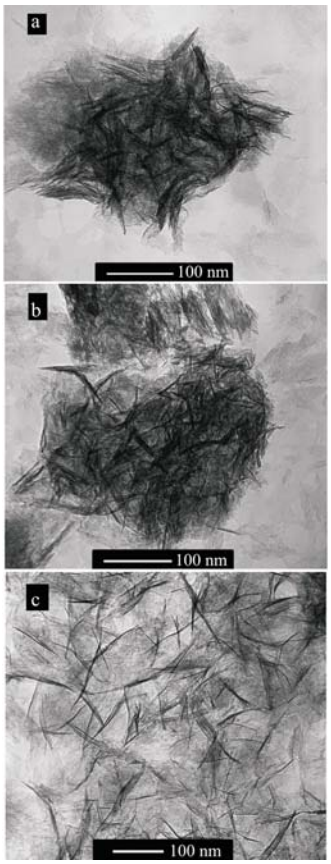

Fig. 2 TEM images of a – 1, b – 3 and c – 5% Y-doped boehmite nanofibres

Thermogravimetric analysis

The dynamic thermal analysis of boehmite is displayed in Fig. 3. The results of the dynamic experiment are reported in Table 2. Due to a yttrium rich phase formed in the 10% sample, samples with added yttrium percentage of 1, 3 and 5 were selected for further investigation by dynamic and controlled rate thermogravimetric techniques. The dynamic thermal analyses of the 1, 3 and 5% yttrium doped boehmite are shown in Figs 4–6. The controlled rate thermal analysis of boehmite is displayed in Fig. 7. The controlled rate thermal analysis of 1, 3 and 5% yttrium doped boehmite are displayed in Figs 8–10. The results of the thermal decomposition of the 1, 3 and 5% yttrium doped boehmite are reported in Table 3.

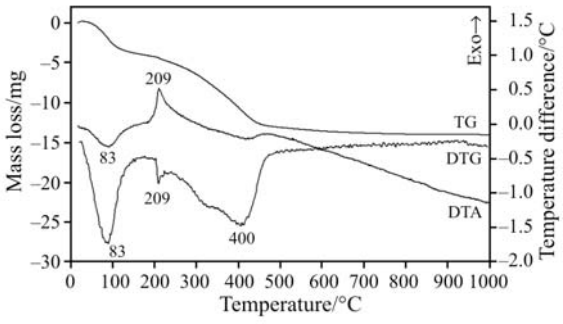

Fig. 3 Dynamic thermal analysis patterns of boehmite

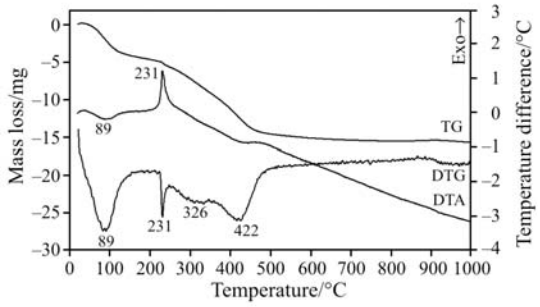

Fig. 4 Dynamic thermal analysis patterns of 1% yttrium doped boehmite

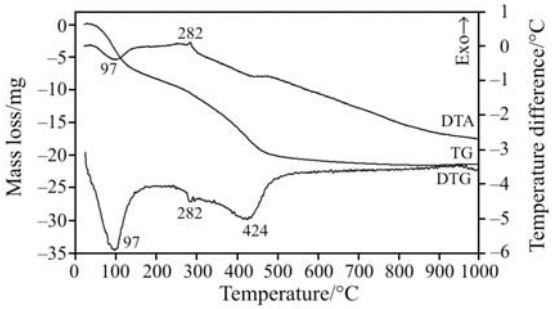

Fig. 6 Dynamic thermal analysis patterns of 5% yttrium doped boehmite

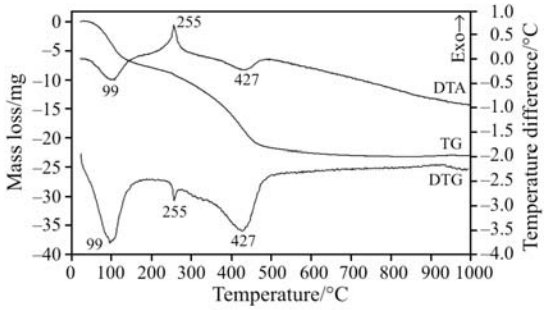

Fig. 5 Dynamic thermal analysis patterns of 3% yttrium doped boehmite

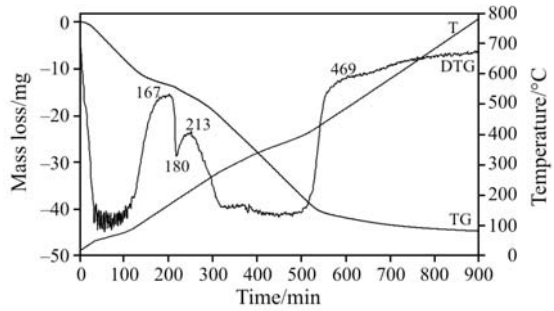

Fig. 7 Controlled rate thermal analysis patterns of 1% yttrium doped boehmite

Pure boehmite with 6 days hydrothermal treatment at 100°C shows four decomposition steps. The step characteristic of boehmite is the broad DTG step at ~397°C with a mass loss of 15.10% (Table 2). The first mass loss occurs at around 83°C with a mass loss of 7.90%. This mass loss step is attributed to adsorbed and intercalated water. The second mass loss step is observed at 209°C and accounts for the major mass loss step of 2.10% mass loss. This mass loss is attributed to interstitial water trapped between the boehmite layers. The theoretical mass loss based upon the equation:

$$2AlOOH \rightarrow Al_2O_3 + H_2O$$

is 15.0% [30].

Undoped boehmite nanofibres/tubes prepared at 100°C for 6 days show at least four separate decomposition steps. The step which is characteristic of boehmite is the sharp DTG step at 345°C, with a mass loss of 13.23%. The first mass loss occurs at around 50°C, with a mass loss of 1.23%. This mass loss step is attributed to adsorbed water. The second mass loss step is observed in the 176–241°C temperature range and accounts for the major mass loss step with 13.24% mass loss. This mass loss is attributed to the combustion of the surfactant [31].

The 1% Y-doped boehmite DTG curve displays 4 maxima in the DTG curves at 89, 231 (sharp), 326 and 422°C. These DTG peaks are assigned to 9a) dehydration (b) combustion of the surfactant directing agent (c) dehydroxylation of boehmite and (d) further dehydroxylation. The DTA curve for this material shows an endotherm at 89 and around 430 and

Table 2 Decomposition stages under dynamic condition for yttrium doped boehmite

Sample											
Boehmite at 100°C			Boehmite 1% Y-doped			Boehmite 3% Y-doped			Boehmite 5% Y-doped		
T_{range}/°C	Mass loss (sample mass: 53.11 mg)/		T_{range}/°C	Mass loss (sample mass: 56.91 mg)/		T_{range}/°C	Mass loss (sample mass: 88.85 mg)/		T_{range}/°C	Mass loss (sample mass: 76.02 mg)/	
	mg	%		mg	%		mg	%		mg	%
24–172	4.2	7.9	29–205	4.9	8.6	25–199	8.0	9.0	25–211	8.7	11.4
172–246	1.1	2.1	205–256	1.1	1.9	199–270	1.7	1.9	211–305	2.8	3.7
246–506	8.0	15.1	256–360	3.6	6.3	270–516	12.3	13.8	305–527	9.1	12.0
506–877	0.9	1.7	360–500	5.1	9.0	516–800	1.2	1.4	527–800	1.1	1.4
			500–800	0.9	1.6						

Table 3 Decomposition stages under CRTA conditions for 1, 3 and 5% Y-doped boehmite

Decomposition process	T_{range}/°C	Mass loss (sample mass: 160.00 mg)/		T_{range}/°C	Mass loss (sample mass: 215.14 mg)/		T_{range}/°C	Mass loss (sample mass: 237.99 mg)/		T_{range}/°C	Mass loss (sample mass: 189.03 mg)/	
		mg	%		mg	%		mg	%		mg	%
Dehydration	22–167	13.4	8.4	22–175	17.9	8.3	21–172	23.5	9.9	22–193	22.6	12.0
Dehydration	167–213	2.2	1.4	175–326	17.4	8.1	172–480	38.2	16.1	193–508	30.2	16.0
Dehydroxylation	213–469	25.8	16.1	326–474	21.2	9.9	480–620	2.9	1.2	508–716	2.3	1.2
	469–764	3.1	1.9	474–667	3.2	1.5						

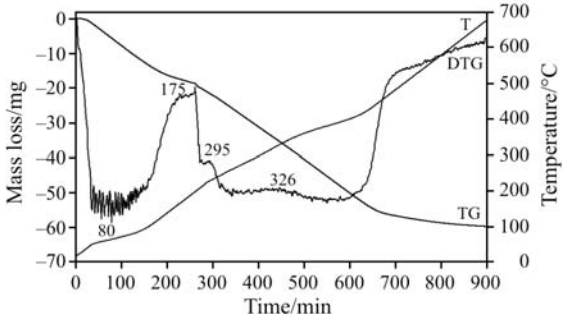

Fig. 8 Controlled rate thermal analysis patterns of 1% yttrium doped boehmite

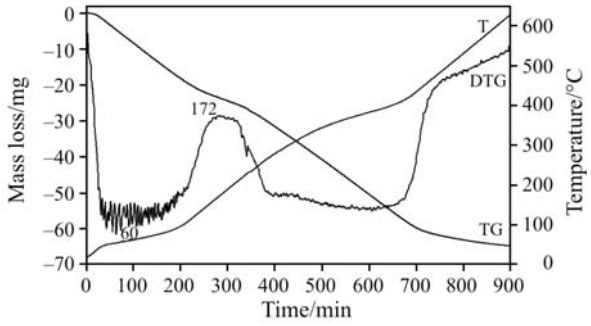

Fig. 9 Controlled rate thermal analysis patterns of 3% yttrium doped boehmite

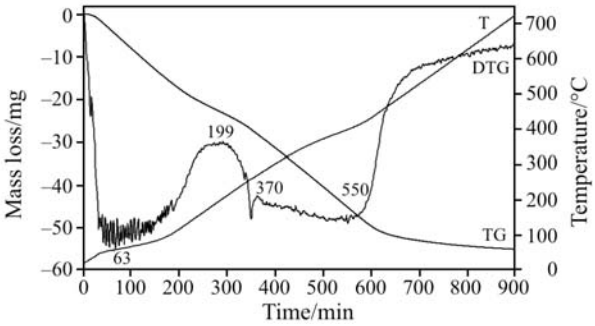

Fig. 10 Controlled rate thermal analysis patterns of 5% yttrium doped boehmite

an exotherm at 231°C. It is proposed that at 427°C the boehmite nanofibres transformed to γ-alumina. The DTG peak and the DTA exotherm at 231°C are assigned to the combustion of the PEO surfactant. In a previous piece of research infrared emission spectroscopy was used to study the dehydroxylation of natural and synthetic boehmite [32]. It was found that dehydroxylation starts at 250 and is complete by 450°C. The dehydroxylation is followed by the loss of intensity of the hydroxyl stretching frequencies observed at 3478, 3319 and 3129 cm^{-1} and by the loss of intensity of the hydroxyl deformation modes at 1140 and 1057 cm^{-1}. A previous study made simulations of the thermal decomposition of boehmite [33]. It was found that the simulations of the non-isothermal experiments. at constant heating rates show that thermally stimulated transformation of nanocrystalline boehmite into alumina can be accurately modelled by a 4-reaction mechanism involving: (I) the loss of physisorbed water, (II) the loss of chemisorbed water, (III) the conversion of boehmite into transition alumina, (IV) the dehydration of transition alumina (loss of residual hydroxyl groups) [33]. Another study of boehmite precipitates by the authors found that thermal analysis showed five endotherms at 70, 140, 238, 351 and 445°C and these endotherms are attributed to the dehydration and dehydroxylation of the hydrolyzate [34].

The calculation of the water content is given in the appendix. For the 1% yttrium doped boehmite the amount of water was calculated as 0.30 mol mol^{-1} of AlO(OH). The values for 3 and 5% yttrium doped boehmite are 0.36 and 0.45 moles of water per mole of AlO(OH). The relationship between the moles of water in the interlayer and the moles of yttrium doping of the boehmite appears linear. The relationship is given as $y=0.375x+0.2575$ with $R^2=0.9868$. In a previous study the authors proposed that water was incorporated into the boehmite structure through folding of the boehmite layers which resulted in changes in the 020 reflection [34]. It was postulated that the structure of the resultant AlO(OH) formed from cold water hydrolysis of trisecbutoxyaluminium(III) was one of folded boehmite structure along the 020 planes of boehmite. This structure was then proposed to straighten during ageing of the amorphous aluminium oxy(hydroxide), which results in the formation of pseudoboehmite. Such a structure showed an X-ray diffraction pattern with the (020) peak for pseudoboehmite but not other peaks, which was attributed to the disintegration of long range order but preservation of short range order. It should be noted that the temperature of hydrolysis is 75°C. The reason for the selection of this temperature is that at and above this temperature a single phase is formed. If the hydrolysate is formed at 25°C, an amorphous aluminium oxy(hydroxide) is formed, which on ageing transforms to boehmite and gibbsite. Thus it is proposed that the increase in Y-content in the boehmite results in an increase in the amount of pseudoboehmite and thus more water is incorporated into the pseudoboehmite structure.

The 3% Y doped boehmite shows three DTG peaks at 99, 255 and 427°C. The DTA curve displays two endotherms at 99 and 427°C and an exotherm at 255°C.

The attribution of the DTG peaks is as above. The 5% Y-doped boehmite shows three DTG peaks at 97, 282 and 424°C. The DTA curve of the 5% Y-doped boehmite displays two endotherms at 97 and 427°C and an exotherm at 282°C. It appears that as the yttrium dop-

ing increases the DTG peak at around 427°C becomes significantly broader. This provides an indication of the wide range of nanofibres present in the boehmite nanomaterial. In the work reported by Alphonse and Courty [33] the DTG peak for the nanocrystalline boehmite of platelets of size 10 nm was around 390°C. It is concluded that the boehmite nanofibres produced in this research thermally transform at higher temperatures than boehmite crystals and boehmite platelets.

The CRTA of the pure boehmite (Fig. 7) shows as for the dynamic experiment shows four decomposition steps as per Table 3. These steps are attributed to two dehydration steps the first of which is isothermal at ~70°C and is assigned to adsorbed water. This accounts for a 8.4% mass loss. The second mass loss at 180°C is obviously non-isothermal and accounts for a 1.4% mass loss. In the dynamic experiment a significant exothermic reaction was observed at 209°C. The third mass loss of 16.10% is also isothermal and occurs at ~400°C. In the dynamic experiment a slow mass loss over a wide temperature range occurs, commencing at around 250 and is complete by 470°C.

The CRTA of the 1% yttrium doped boehmite shows a quasi-isothermal dehydration step at 80°C. Similarly to the dynamic experiment, two dehydroxylation stages can be separated in the 175 to 500°C range with the local minimum in the DTG curve at 326°C. Interestingly, the second step of dehydroxylation is approaching a quasi-isothermal course. The shoulder in the DTG curve at about 220°C is assigned to the combustion of traces of the surfactant adsorbed on the surface.

The CRTA of the 3% yttrium doped boehmite shows a quasi-isothermal step of dehydration at around 60°C. The two-stage pattern of dehydroxylation can also be observed in the DTG curve in the 175 to 450°C range. The second (quasi-isothermal) step of dehydroxylation is increased at the expense of the first one. The burning of the surfactant can also be identified at around 220°C. The CRTA of the 5% yttrium doped boehmite shows a quasi-isothermal dehydration step at about 63°C. The combustion of the surfactant can be observed at about 250°C. Although the second part of dehydroxylation is approaching a quasi-isothermal pattern, the separation of the two dehydroxylation processes can no longer be observed in the DTG curve. This is in harmony with the dynamic experiments. In the dynamic experiments the two dehydroxylation steps at 326 and 422°C gradually merged with the increase of yttrium concentration. The anomaly why the initial part of dehydroxylation is non-isothermal, while the second part is getting to be an isothermal process needs further studies on the mechanism of decomposition.

Conclusions

Yttrium doped boehmite nanofibres of some 250 nm in length can be prepared at 100°C using soft chemical hydrothermal methodology using PEO as a surfactant directing agent. The yttrium content in boehmite nanostructures was found to be limited to a maximum of around 5.0%. Fibres or needles were formed at low Y-doping. With the increasing Y-content nanosheets are formed.

Thermal analysis under dynamic and CRTA conditions shows that the steps of dehydroxylation are merged with the increase of the yttrium content. The CRTA experiment revealed that the two steps of dehydroxylation take place according to different mechanisms.

Appendix

Calculation of water content for Y-doped boehmite

using the formula $AlO(OH)\cdot xH_2O$. Loss of water is calculated according to the reaction:

$$AlO(OH)\cdot xH_2O \rightarrow AlO(OH)+xH_2O$$

A) 1% Y-doped boehmite

Composition: $AlO(OH)\cdot xH_2O$

Loss of water up to 175°C is 17.9 mg (0.993 mmol).
Mass of dehydrated mineral is 197.24 mg (3.288 mmol).
Thus, the amount of crystallization water is 0.30 mol.

B) 3% Y-doped boehmite

Composition: $AlO(OH)\cdot xH_2O$

Loss of water up to 172°C is 23.5 mg (1.304 mmol).
Mass of dehydrated mineral is 214.49 mg (3.575 mmol).
Thus, the amount of crystallization water is 0.36 mol.

C) 5% Y-doped boehmite

Composition: $AlO(OH)\cdot xH_2O$

Loss of water up to 193°C is 22.6 mg (1.254 mmol).
Mass of dehydrated mineral is 166.43 mg (2.774 mmol).
Thus, the amount of crystallization water is 0.45 mol.

Acknowledgements

The financial and infra-structure support of the Queensland University of Technology Inorganic Materials Research Program of the School of Physical and Chemical Sciences is gratefully acknowledged. The Australian Research Council (ARC) is thanked for funding the Thermal Analysis facility through a LIEF grant. One of the authors (YZ) is thankful for a Queensland University of Technology international doctoral scholarship (QIDS).

References

1 J. H. Fendler and F. C. Meldrum, Adv. Mater. (Weinheim, Germany), 7 (1995) 607.
2 B. B. Lakshmi, C. J. Patrissi and C. R. Martin, Chem. Mater., 9 (1997) 2544.
3 Y. Sun and Y. Xia, Nature, 298 (2002) 2176.
4 M. S. Gudiksen, L. J. Lauhon, J. Wang, D. C. Smith and C. M. Lieber, Nature, 415 (2002) 617.
5 C. Kaya, J. Y. He, X. Gu and E. G. Butler, Microporous Mesoporous Mater., 54 (2002) 37.
6 Y. Zhao, W. N. Martens, R. L. Frost and H. Y. Zhu, Langmuir, 23 (2007) 9850.
7 H. Y. Zhu, X. P. Gao, D. Y. Song, S. P. Ringer, Y. X. Xi and R. L. Frost, Microporous Mesoporous Mater., 85 (2005) 226.
8 H. Y. Zhu, J. D. Riches and J. C. Barry, Chem. Mater., 14 (2002) 2086.
9 J.-L. Le Loarer, H. Nussbaum and D. Bortzmeyer, Alumina Extrudates, Methods for Preparing and Use as Catalysts or Catalyst Supports, (Rhodia Chimie, Fr.), Application: WO, 1998, p. 44.
10 V. S. Burkat, V. S. Dudorova, V. S. Smola and T. S. Chagina, Light Metals, Warrendale, PA, USA 1985, pp. 1443–1448.
11 C. Nedez, J.-P. Boitiaux, C. J. Cameron and B. Didillon, Langmuir, 12 (1996) 3927.
12 Y. Chen, L. Jin and Y. Xie, J. Sol-Gel Sci. Technol., 13 (1998) 735.
13 D. S. Xue, Y. L. Huang, Y. Ma, P. H. Zhou, Z. P. Niu, F. S. Li, R. Job and W. R. Fahrner, J. Mater. Sci. Lett., 22 (2003) 1817.
14 A. P. Philipse, A.-M. Nechifor and C. Patmamanoharan, Langmuir, 10 (1994) 4451.
15 K. Okada, A. Tanaka, S. Hayashi, K. Daimon and N. Otsuka, J. Mater. Res., 9 (1994) 1709.
16 S. Ananthakumar, V. Raja and K. G. K. Warrier, Mater. Lett., 43 (2000) 174.
17 A. H. Heuer, N. J. Tighe and R. M. Cannon, J. Am. Ceram. Soc., 63 (1980) 53.
18 J. Cho, M. P. Harmer, H. M. Chan, J. M. Rickman and A. M. Thompson, J. Am. Ceram. Soc., 80 (1997) 1013.
19 J. M. Bouzaid, R. L. Frost, A. W. Musumeci and W. N. Martens, J. Therm. Anal. Cal., 86 (2006) 745.
20 R. L. Frost, J. M. Bouzaid, A. W. Musumeci, J. T. Kloprogge and W. N. Martens, J. Therm. Anal. Cal., 86 (2006) 437.
21 R. L. Frost, J. Kristóf, W. N. Martens, M. L. Weier and E. Horváth, J. Therm. Anal. Cal., 83 (2006) 675.
22 R. L. Frost, A. W. Musumeci, J. T. Kloprogge, M. L. Weier, M. O. Adebajo and W. Martens, J. Therm. Anal. Cal., 86 (2006) 205.
23 R. L. Frost, R.-A. Wills, J. T. Kloprogge and W. Martens, J. Therm. Anal. Cal., 84 (2006) 489.
24 R. L. Frost, R.-A. Wills, J. T. Kloprogge and W. N. Martens, J. Therm. Anal. Cal., 83 (2006) 213.
25 R. L. Frost, J. Kristóf, M. L. Weier, W. N. Martens and E. Horváth, J. Therm. Anal. Cal., 79 (2005) 721.
26 R. L. Frost, M. L. Weier and W. Martens, J. Therm. Anal. Cal., 82 (2005) 115.
27 R. L. Frost, M. L. Weier and W. Martens, J. Therm. Anal. Cal., 82 (2005) 373.
28 Y.-H. Lin, M. O. Adebajo, R. L. Frost and J. T. Kloprogge, J. Therm. Anal. Cal., 81 (2005) 83.
29 Y. Zhao, R. L. Frost, W. N. Martens and H. Y. Zhu, Langmuir, 23 (2007) 9850.
30 Y. Zhao, R. L. Frost, W. N. Martens and H. Y. Zhu, J. Therm. Anal. Cal., 90 (2007) 755.
31 Y. Zhao, R. L. Frost and W. N. Martens, J. Phys. Chem., C 111 (2007) 5313.
32 R. L. Frost, J. T. Kloprogge, S. C. Russell and J. Szetu, Appl. Spectrosc., 53 (1999).
33 P. Alphonse and M. Courty, Thermochim. Acta, 425 (2005) 75.
34 W. N. Martens, R. L. Frost, J. Bartlett and J. T. Kloprogge, Thermochim. Acta, 374 (2001) 31.

Received: January 14, 2008
Accepted: April 1, 2008
OnlineFirst: August 15, 2008

DOI: 10.1007/s10973-008-9002-6